Journal of Geophysical Research: Space Physics

RESEARCH ARTICLE
10.1002/2017JA025106

Key Points:
- We survey persistent, intense upward MeV electron beams in Jupiter's polar regions
- These intense beams appear to be well correlated with the swirl region of the Jovian aurora
- We consider Juno JEDI data from perijove 1 through perijove 8

Intervals of Intense Energetic Electron Beams Over Jupiter's Poles

C. Paranicas[1], B. H. Mauk[1], D. K. Haggerty[1], G. Clark[1], P. Kollmann[1], A. M. Rymer[1], B. Bonfond[2], W. R. Dunn[3], R. W. Ebert[4], G. R. Gladstone[4], E. Roussos[5], N. Krupp[5], F. Bagenal[6], S. M. Levin[7], J. E. P. Connerney[8], and S. J. Bolton[4]

[1]APL, Laurel, MD, USA, [2]Technologies and Astrophysics Research Institute, Université de Liège, Liège, Belgium, [3]MSSL, Department of Space and Climate Physics, UCL, Dorking, UK, [4]SWRI, San Antonio, TX, USA, [5]MPS, Goettingen, Germany, [6]Laboratory for Atmospheric and Space Physics, University of Colorado Boulder, Boulder, CO, USA, [7]JPL, Pasadena, CA, USA, [8]GSFC, Greenbelt, MD, USA

Abstract Juno's Jupiter Energetic particle Detector Instrument often detects energetic electron beams over Jupiter's polar regions. In this paper, we document a subset of intense magnetic field-aligned beams of energetic electrons moving away from Jupiter at high magnetic latitudes both north and south of the planet. The number fluxes of these beams are often dominated by electrons with energies above about 1 MeV. These very narrow beams can create broad angular responses in the Jupiter Energetic particle Detector Instrument with unique signatures in the detector count rates, probably because of >10 MeV electrons. We use these signatures to identify the most intense beams. These beams occur primarily above the swirl region of the polar cap aurora. This polar region is described as being of low brightness and high absorption and the most magnetically "open" at Jupiter.

Plain Language Summary We find that there are very intense beams of energetic (probably dominated by >1 MeV) electrons moving upward over Jupiter's north and south poles that are likely to be magnetically connected to the swirl region in the aurora. We use data from Juno's Jupiter Energetic particle Detector Instrument to characterize the upward beams and also present Ultraviolet Spectrograph data showing the swirl region in a color ratio. We have created a table of times when these very intense beams are present from the first through the eighth perijove pass of the spacecraft.

Correspondence to:
C. Paranicas,
chris.paranicas@jhuapl.edu

Citation:
Paranicas, C., Mauk, B. H., Haggerty, D. K., Clark, G., Kollmann, P., Rymer, A. M., et al. (2018). Intervals of intense energetic electron beams over Jupiter's poles. *Journal of Geophysical Research: Space Physics*, *123*, 1989–1999. https://doi.org/10.1002/2017JA025106

Received 6 DEC 2017
Accepted 8 MAR 2018
Accepted article online 12 MAR 2018
Published online 25 MAR 2018

1. Introduction

The Juno spacecraft began to orbit Jupiter in early July 2016. Juno's high inclination orbit allows its instruments to directly sample the fields and particles environment at very high latitude near the planet. Connerney, Adriana, et al. (2017) surveyed the magnetometer, plasma, waves, and energetic charged particle data obtained during the first perijove pass ("PJ1"). Mauk et al. (2017a) presented Jupiter Energetic particle Detector Instrument (JEDI) data obtained over Jupiter's north and south poles and documented mono-directional and bi-directional charged particle beams. Allegrini et al. (2017) concentrated on electron beams in the 100 eV to 100 keV energy range using data from Juno's Jovian Auroral Distributions Experiment (JADE). Clark et al. (2017) used signatures in the Juno data to describe acceleration mechanisms in the polar regions. Ebert et al. (2017) looked at mono-directional and bi-directional beams below 100 keV in energy for several Juno perijoves and characterized their associated energy flux. Electron beams in the tens to hundreds of keV were also observed at high Jovian latitude by the Ulysses spacecraft (e.g., Lanzerotti et al., 1992).

Terrestrial auroral observations provide a basis for interpreting some, but not all, of the measurements in Jupiter's polar regions. In particular, some of the emissions associated with very high energy particles have no Earth analog. For example, Haggerty et al. (2017) described the precipitation of energetic heavy ions at Jupiter that are the presumptive source of the Jovian X-ray auroral line emissions (Branduardi-Raymont et al., 2007; Elsner et al., 2005).

Allegrini et al. (2017), Ebert et al. (2017), and Mauk et al. (2017b) mainly analyzed beams of electrons with energies of up to 100 keV (in the case of the Juno JADE data) and into the few hundreds of keV from JEDI. But further investigation suggests that electron beams can extend well into the MeV energy range. How electrons can be accelerated into the MeV energy range at very low Jovian altitudes is a mystery. The beams we describe here, like those linked to the X-ray emissions, are believed to be

on field lines poleward of the main aurora and therefore are connected to regions beyond the middle magnetosphere.

In this paper, we focus on field-aligned distributions in the JEDI data. JEDI nominally detects electrons from 30 to 800 keV (with some sensitivity below 30 keV and up to about 1.2 MeV) using three units rigidly mounted onto the spacecraft with no means of articulation beyond that provided by spacecraft rotation. These units are referred to here as, *JEDI-90*, *JEDI-A180*, and *JEDI-270*, following the instrument paper, Mauk, Haggerty, Jaskulek, et al. (2017). In their high-resolution modes, these units each provide six 12° × 18° fields of view (FOVs), so that different local pitch angles are sampled at every instant of time. When combined with the spacecraft's 30 s spin period, a more complete range of local pitch angles can often be sampled. Pitch angle information is computed using Juno vector magnetometer observations (Connerney, Benn, et al., 2017).

JEDI combines thin foils, microchannel plate sensors, and solid-state detectors (SSDs) to measure both electrons and ions with energies greater than about 20 keV (Mauk, Haggerty, Jaskulek, et al., 2017) and makes coincident ion measurements. The coincidence requires, for example, a start and stop pulse triggered by the ion in order for it to be counted, thus reducing the probability of false counts. Electrons, however, are measured with the SSDs alone; interpreting their responses can be challenging in regions where electron energies are particularly high. The "ion" SSDs are essentially bare detectors responsive to ions and electrons that deposit more energy than required by the threshold setting (~20 keV). It is frequently the case at Jupiter that the JEDI *ion* SSDs are dominated by electron counts. The "electron" SSD's reside behind a small flashing (2 μm of aluminum) and are mostly responsive to >30 keV electrons, > 250 keV protons, and even more energetic heavy ions.

By comparing the coincident ion measurements and the SSD responses, we have concluded that the SSD responses are excited primarily by electrons for events analyzed in this paper. Also, when the JEDI-A180 sensor is configured to use its small SSD pixels rather than its large pixels (see, Mauk, Haggerty, Jaskulek, et al., 2017), two of the six ion detectors act as "witness" detectors, because they are located behind a shield made of about 635 μm of titanium. The shield prevents electrons below about 700 keV (and ions to a much higher energy cutoff) from reaching the detectors directly (due to electron scattering within the shield, shielding effectiveness is statistical in nature). The two shielded detectors are JEDI-A180 SSD1 and SSD3 (in small pixel ion mode only) out of the array of six SSDs, numbered SSD0–SSD5. Note that JEDI-90 and JEDI-270 do not have witness detectors. The response of these witness detectors must be interpreted with care, because about 8% of foreground electrons can reach the shielded detectors, owing to spacing between the shields and the detectors and electron scattering. A thorough description of JEDI is provided in Mauk, Haggerty, Jaskulek, et al. (2017), and the flashing and witness information and its impact on measurements are described further in Paranicas et al. (2017).

2. Observations of Energetic Upward Beams

Figure 1 shows JEDI measurements obtained during PJ1. The first panel shows JEDI count rates, summed over energy, from the electron SSDs as a function of time and local pitch angle. In Figure 1 we have excluded the three lowest energy channels (energies below 30 keV) from this sum to minimize counts obtained near the detector thresholds. As is usually the case during perijove passes, all three JEDI's were obtaining data using the electron detectors around PJ1. The middle three panels show combined count rate data from the electron detectors on all the JEDI units as a function of energy. The data are separated so that each panel shows a narrow range of local pitch angles: the second panel shows particles moving parallel to the magnetic field, the third panel shows particles with nearly 90° local pitch angles, and the fourth panel shows particles moving antiparallel to the magnetic field direction. The fifth panel shows the "singles" rates (total rates on the detectors above each of their energy thresholds) for the JEDI-A180 ion detectors. Note that two of the traces shown there, SSD1 and SSD3, represent the response of the witness detectors described above. One of the JEDI-A180 detectors (SSD0) is partially blocked by the collimator.

In this paper, we focus on upward energetic electron beams observed over an extended spatial region before and after Juno perijoves. These beams occur at higher magnetic latitudes than the very high latitude portion of the main radiation belts. These radiation belt crossings at high latitude in the north and the south can be identified in the plot as the most intense periods, such as around the peaks in the lower panel between 12:00 and 13:30 UTC. During the inbound portion of PJ1, there are traces of an upward beam beginning just after 10:00 and extending to just after 12:00 and from about 13:40 onward in the outbound data (see first panel

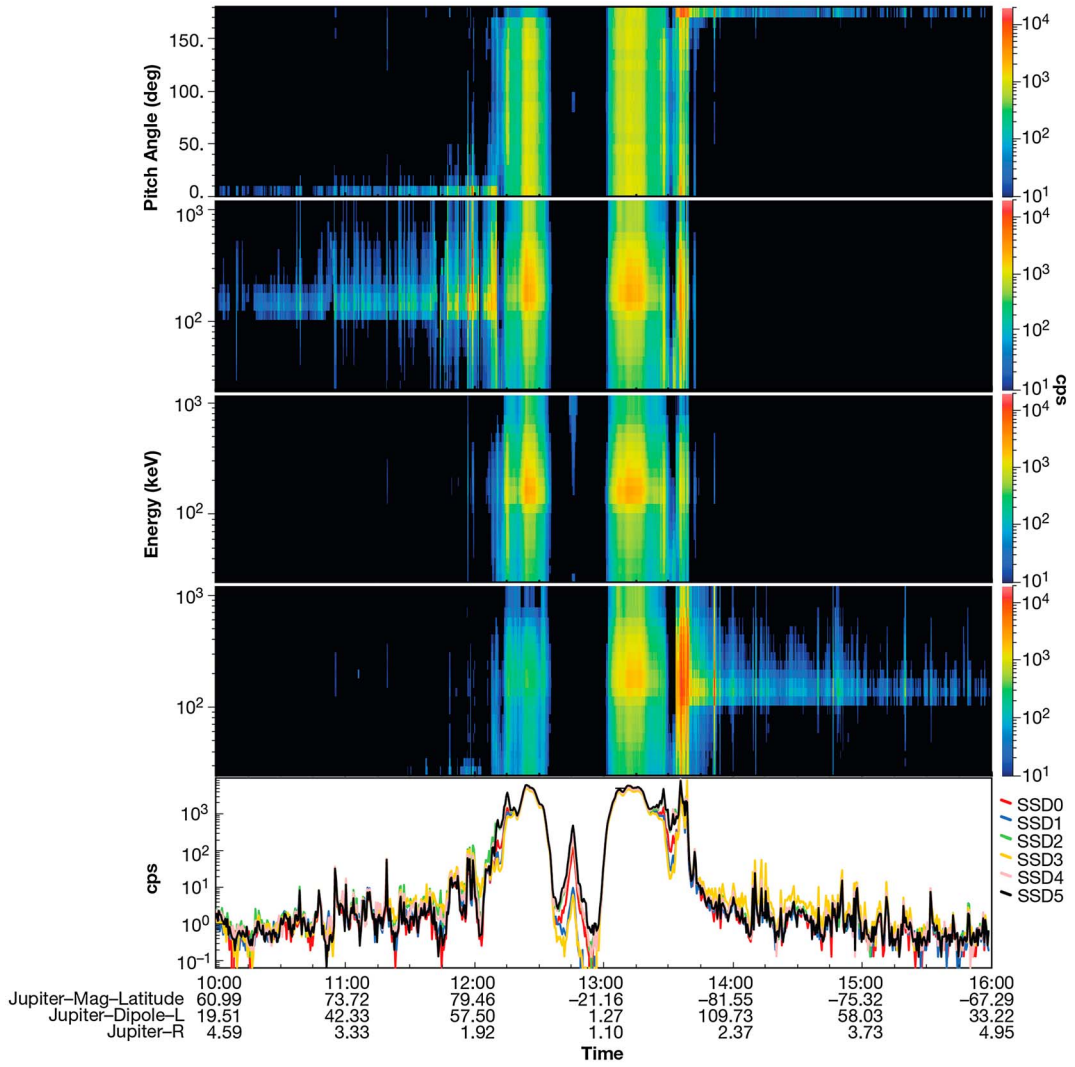

Figure 1. Jupiter Energetic particle Detector Instrument (JEDI) data from day 2016-240 as Juno moves from north to south through PJ1. The first panel shows electron cps versus local pitch angle, combining data from all three JEDIs. The second through fourth panels shows electron cps data from all three JEDIs, now as a function of energy and including only those data taken at local pitch angles of 0–15° (second), 80-100° (third), and 165–180° (fourth). The fifth panel shows r-versus-r corrected singles rates from the JEDI-A180 small pixel ion solid-state detectors (SSDs) (each SSD cps is a separate line).

near 0° and near 180°). When separated by pitch angle (middle three panels), the times of the upward beams usually show a band centered around ~160 keV when the detector looks into the beam (second panel from the top inbound and fourth panel from the top outbound). The band varies in intensity. The intermittent nature of this band is partly due to the rotation of the JEDI FOVs into and out of the beam direction. Lastly, we would like to point out that by comparing Figure 1 here with Figure 1 of Haggerty et al. (2017), one can see that just before and just after PJ1, energetic ions appear to be precipitating, while energetic electrons are moving away from the planet. Haggerty et al. (2017) do not see significant fluxes of energetic protons in their data that are moving away from Jupiter. This gives us more confidence that the particles measured by the SSDs and described here are electrons. Also, Bunce et al. (2004) have shown that very energetic electrons can be accelerated at high Jovian latitudes away from the planet.

The count rate peak around 160 keV corresponds to the "minimum ionizing energy" of the detector. Electrons with energies greater than about 420 keV begin to fully penetrate the JEDI SSDs. The fraction of particles that fully penetrate has been parameterized as, $f \sim \exp[-2(480/E(\text{keV}))^3]$, the complement to the detection efficiency ($e \sim 1 - f$) provided in Mauk et al. (2017b). JEDI has channels that measure energy deposition to

about 1.2 MeV for electrons but measure electrons with lower efficiency above ~400 keV. At the 10 counts per s (or cps) level, there are periods of time when the band is present, but there are low counts above the band, suggesting that the beam has substantial electron contributions above 1.2 MeV at those times.

The beams seen in Figure 1 generate only a limited response from the detectors when the aperture is viewing pitch angles not aligned with the beam. This observation suggests that the beams are not dominated by particles with sufficient energy (>15 MeV electrons) to penetrate the housing of the instrument or other structures intended to stop the particles. Electrons above ~15 MeV reach the detectors from virtually any direction because the shielding material cannot stop them. These electrons can produce both bremsstrahlung and secondary electrons in the housing that deposit energy in the detector, resulting in false counts. However, the efficiency for counting bremsstrahlung is low and it would not generally create a band at 160 keV. Furthermore, the counts of secondaries would be similar to those of the primaries that cause them. This is because all particles (primaries, secondaries, X-rays, etc.) arrive at the detector within the same time window and so the sensor would view them as if they were a single particle with an energy that is the sum of all of them. Using the arbitrary cutoff of 10 cps shows that neither of these conditions stands out in the data.

Since JEDI can directly detect electrons to about 1.2 MeV, the discussion above suggests that electrons in the beam with energies between 1 and 15 MeV are not uncommon. This seems to agree well with the radiation monitoring system analysis of >5 and >10 MeV electrons presented in Becker et al. (2017), see below. Our analysis does not extend to a more rigorous accounting of the likely energy spread at each time. Mauk et al. (2017a) used the minimum ionizing peak to assess whether the electron energy spectrum is above JEDI's measurement capability. They reasoned that the local maximum in the energy spectrum near 160 keV could be used to constrain the total counts in the high energy tail of the electron distribution, assuming, for example, that the energy spectrum follows a power law to very high energies. Their modeling technique also accommodates a beam energy range that is not characterized by an extended tail but mainly confined between a minimum and maximum energy (e.g., a beam could be entirely between 2 and 4 MeV).

In addition to the time-energy or time-pitch angle spectrograms, the ion SSD singles rates can also be useful for extracting information about the beams. For foreground particles in the tens to several hundreds of keV energy range, the singles rates are often organized as they are near 12:45 (Figure 1, fifth panel) at the position of a local maximum observed near Juno's closest approach to Jupiter (see Kollmann et al., 2017). The two witness-shielded detectors (SSD1 and SSD3) measure the lowest rates, and SSD0, which has some collimator blockage, measures a lower rate than the unobstructed detectors (SSD2, SSD4, and SSD5). These populations close to Jupiter have strongly trapped distributions and one concludes that here the witness shields have stopped some of the measurable particles that would otherwise have reached the detector. However, for other cases, care must be exercised because the ordering of the SSD singles rates can be influenced by the pitch angle distribution. A beam is an extreme example of a nonisotropic distribution and can strongly alter the ordering of the SSD rates. For example, if only one SSD on a JEDI unit views in the beam direction, it can dominate the other SSD rates, even if there is a witness shield in front of the detector. Below about 10 cps, other issues such as threshold settings can also become significant.

3. More Intense Events

Figure 2 shows for PJ3 the same kind of observations as illustrated for PJ1 in Figure 1. The first panel suggests that for both inbound and outbound, the dominant count rates are in the field-aligned direction, but the inbound period is more complicated. The second panel from the top again shows an intense band around 160 keV observed over a large region of space. But unlike in Figure 1, there frequently appears a faint band centered near 160 keV during times when JEDI collects data at other local pitch angles. The first panel also shows that the other pitch angles get some count rates above the 10 cps level at times of the most intense beam detection.

The fifth panel in Figure 2 shows that the JEDI-A180 ion SSDs record fairly different singles count rates prior to about 15:37. After that, the 30 s averaged JEDI-A180 ion singles count rates are fairly similar to each other until about 16:20. Two of the singles detectors are witness detectors, so in principal, the rates should not be the same unless the vast majority of the particles that are detected during this time are easily

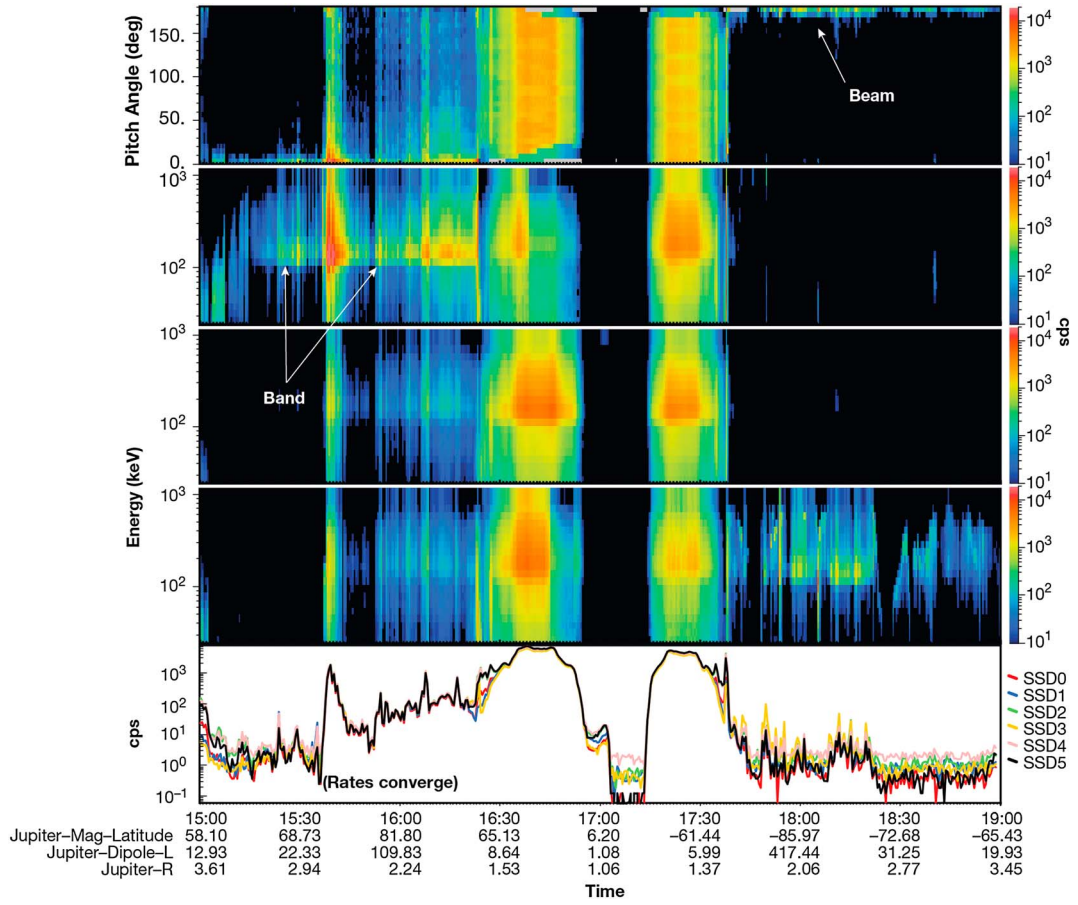

Figure 2. Same display type as Figure 1 for Jupiter Energetic particle Detector Instrument data obtained on day 2016-346, during PJ3. The beam as it would appear in a pitch angle versus time spectrogram, the band at approximately 160 keV, and the times when the singles rates are all about the same (labeled as, "Rates converge") are indicated.

penetrating the witness shield (e.g., >700 keV electrons). Outbound, the situation is very different. On average, the singles rates are lower and the band at 160 keV is virtually absent in look directions other than the upward field-aligned direction, above the 10 cps level. The periods of time when (1) all of the JEDI-A180 ion singles rates are similar to each other (e.g., the fifth panel of Figure 2 showing the period of time when the rates converge) and (2) significant counts are detected when the detector is not pointing into the beam (e.g., the third and fourth panels from the top showing a faint band centered at about 160 keV and spread out in energy) are often the same periods of time. Note also that within the time period we consider here (15:37–16:19), a specific event occurred at 15:40 that was analyzed in Mauk et al. (2017b). At that time, Juno was thought to have crossed a polar auroral arc that may be associated with broadband auroral acceleration from stochastic processes. Ultraviolet Spectrograph (UVS) images in Mauk et al. (2017b) suggest that this arc lies on the border of the swirl region (Grodent et al., 2003).

During the inbound portion of the trajectory shown in Figure 2, the local pitch angle distributions of the ion SSDs (not shown) have the highest intensity when the look direction is closest to local pitch angles of 0°. This observation indicates that the beam dominating the count rate is an upward beam and not the result of false counts from downward MeV ions that are also observed in the polar regions (see, Haggerty et al., 2017). As noted above, energetic ions are detected by JEDI using coincidence, lending support to the conclusion that these are upward moving electrons. Furthermore, the variation with look direction suggests that the beam is not entirely made up of >15 MeV electrons. As we discussed in Paranicas et al. (2017), when >15 MeV electrons are present, they can penetrate the JEDI housing and deposit energy in the detectors. When present in large numbers, the detector response becomes independent of the pitch angle range it is sampling.

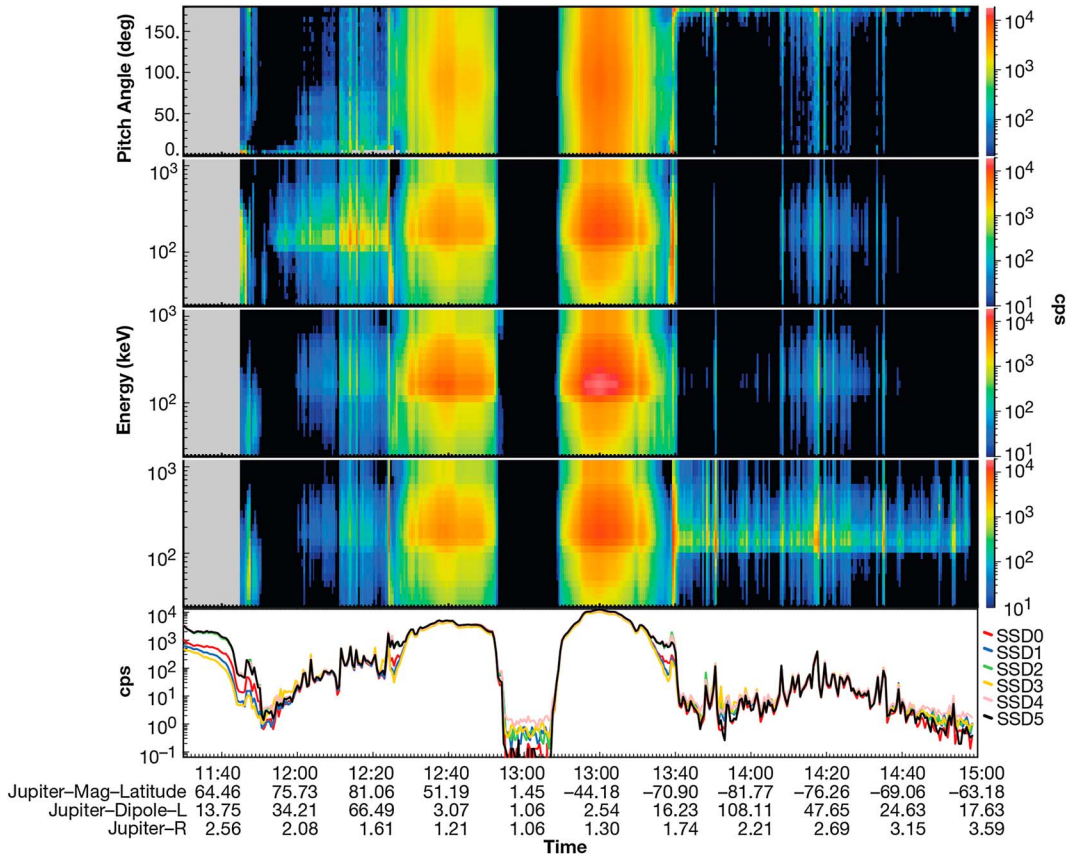

Figure 3. Same display as in Figures 1 and 2 for data obtained on day 2017-033, during PJ4. Note that the ion singles rates (lower panel) have time periods that satisfy the conditions for intense beams both before and after perijove (i.e., in the north and south).

At times (periods with significant ion SSD rates that are all the same and a notable presence of pitch angle scattering in the data), the pitch angle distributions as measured by the electron SSD's appear inconsistent with one another. That is, at the same time and at the same pitch angle, two SSDs sometimes respond with different count rates. Two effects can contribute to such a situation. An intense electron beam that enters the wide collimator of JEDI can scatter internally and deposit energy into nonaligned detectors. Two examples from Mauk et al. (2017a, see their Figure 4) show rates for detectors 90° from the aligned direction, at 2% and 0.3% of those in the aligned direction, presumably depending on how cleanly the beam has entered the collimator. But the second way that inconsistent pitch angle distributions can occur is if the beam contains substantial intensities with energies $>$10 MeV (that can penetrate the collimator blades) and $>$ 15 MeV (that can penetrate the housing) such that the directionality of the detector response depends on shielding geometries that include the complicated structure of the spacecraft. The occurrence of this second contribution to anomalous pitch angle distributions was clearly demonstrated in Jupiter's radiation belt horns by Paranicas et al. (2017). The band around 160 keV offers some guidance that these beams must contain high energy components. Additionally, radiation monitoring data presented by Becker et al. (2017) show a period of $>$10 MeV electrons that agrees well with the times of the intense beam predicted by JEDI on the inbound leg of PJ3.

To summarize these points, we propose that the strength of the upward electron beams can be understood as follows. The presence of the band around 160 keV is indicative of $>$420 keV electrons, and the intensity and spread around this energy (i.e., 160 keV) indicate the presence of weaker or stronger beams. Since JEDI can directly make measurements to 1.2 MeV, the lack of clear signal below that cutoff means there are substantial contributions to these intense beams above about 1 MeV. The near equality of the JEDI-A180 small ion pixel singles rates can be used to discriminate between energetic beams and the most intense beams (i.e., likely a combination of number flux and energy range).

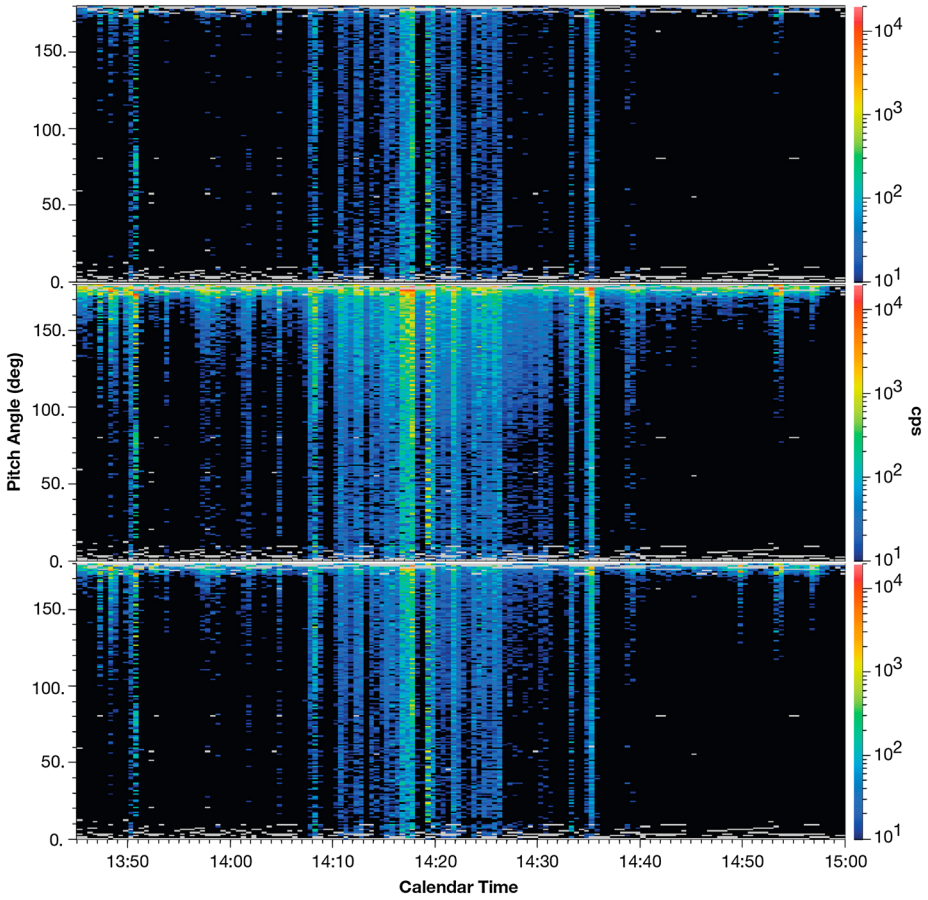

Figure 4. Electron count rate data summed over several energy channels versus local pitch angle using data from all three Jupiter Energetic particle Detector Instruments obtained on day 2017-033, during PJ4. The spacecraft was over the southern hemisphere of Jupiter, and the higher count rates near local pitch angles of 180° suggest an upward beam. The approximate energy ranges of the panels are (top) 25–78, (middle) 71–270, and (bottom) 260–1215 keV. The middle panel would contain the main contributions from the band at about 160 keV.

4. Other Time Periods and Beam Displays

Intense beam regions were observed during PJ4 as well. Figure 3 shows the same kinds of displays as in Figures 1 and 2. For PJ4, the JEDI-A180 ion SSD singles rates are all very similar to each other (i.e., our metric for intense beams) between 12:00 and 12:22 and also between 14:07 and 14:35. This flyby illustrates that the intense upward beams highlighted in this paper (not just the nominal ones as shown for PJ1) occur in high latitude regions in both the north and the south.

In choosing the times of the most intense beams, we select those in which the main particles are field-aligned and there is some presence of the band near 160 keV when detectors are viewing in the assumed beam direction. During the most intense segments of these beams, there are also counts at other pitch angles that are frequently correlated to peaks in the intensity in the field-aligned direction (see first panel). It is possible that these counts are anomalous and due to scattering within JEDI, but they might also be associated with housing-penetrating electrons that are present in low numbers. The presence of counts near 160 keV in the local pitch angle plots that do not correspond to the beam direction may support this hypothesis (middle three panels).

In Figure 4, we show a portion of the data acquired during the intense beam observed outbound, but now separating the count rates into three energy bins with the approximate energy ranges: 25–78, 71–270, and 260–1215 keV. The middle panel with the highest count rates (energy range ~71–270 keV) represents the energies that would be in the band around 160 keV. Between about 13:52 and 14:07 (and again on the

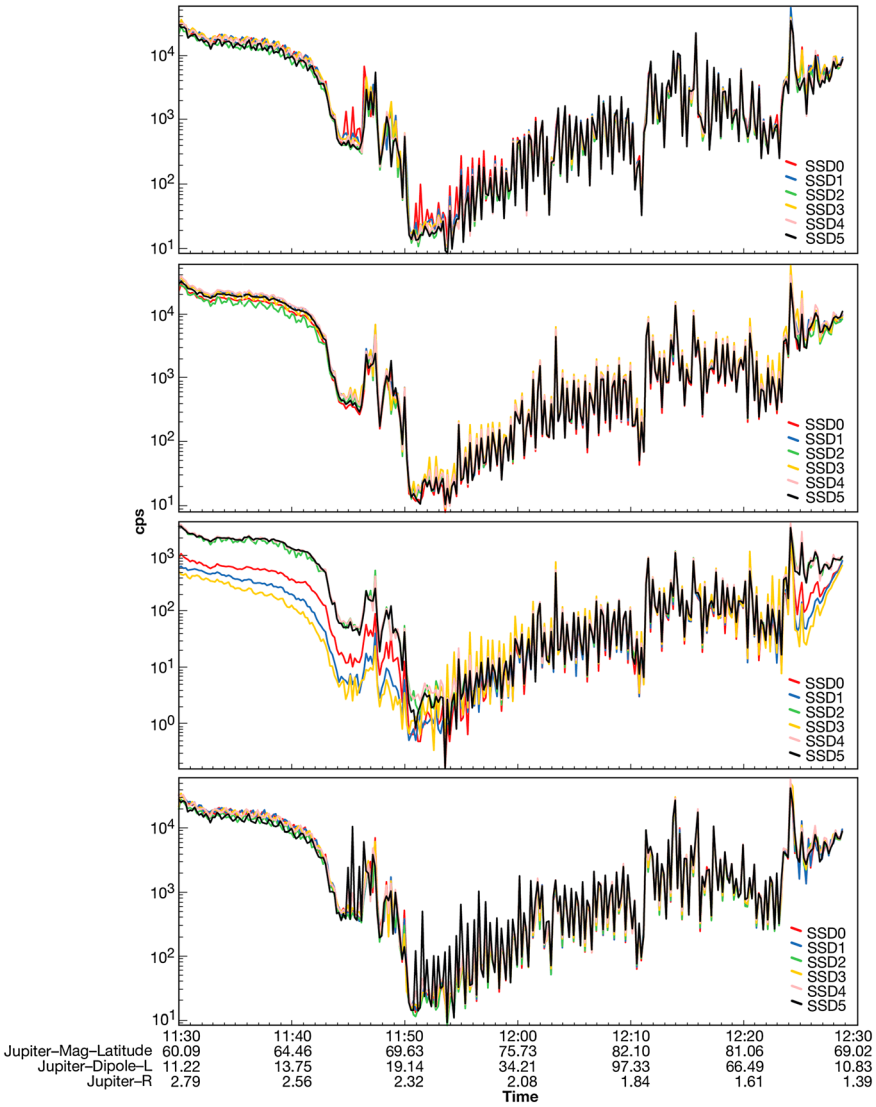

Figure 5. Jupiter Energetic particle Detector Instrument (JEDI) data obtained on day 2017-033 during PJ4. Each panel shows r-versus-r corrected singles counts per second with (first panel) JEDI-90 electrons, (second panel) JEDI-A180 electrons, (third panel) JEDI-A180 ions, and (fourth panel) JEDI-270 electrons. The data are 12 s averaged, and each individual line represents the cps of a single solid-state detector (SSD).

right-hand side of the plot) there are robust counts in the bottom two panels near 180° and some pitch angle scattering. Between 14:11 and 14:26, the pitch angle scattering covers nearly the whole range at the 10 cps level and even the lower energies (top panel) are affected.

In Figure 5, we again show PJ4 data, but this time, it is the singles rates from all three JEDI units. These singles rates are r-versus-r corrected in a standard procedure to restore the true rate from the measured rate at high count rate levels (e.g., Armstrong et al., 1981). Three panels show the output of electron SSDs (panels 1, 2, and 4) and one panel shows ion SSD outputs (panel 3). During PJ4, only the JEDI-A180 ion SSD singles were in small pixel mode, so the singles count rates on the others are about an order of magnitude higher due to the ratio of detector pixel sizes (see, Mauk, Haggerty, Jaskulek, et al., 2017). In the third panel from the top, it is easy to see the progression into the most intense beams. Prior to ~11:53 UTC, the witness rates (SSD1 and SSD3) are well below the other rates. Just after 11:53 UTC, the rates on JEDI-A180 become similar to each other, but SSD3 is still slightly higher (SSD3 is the sector closest to the beam). Later, all sectors measure about the same count rate. When sectors are overwhelmed by the beams, they are often measuring slightly different rates, as we show next.

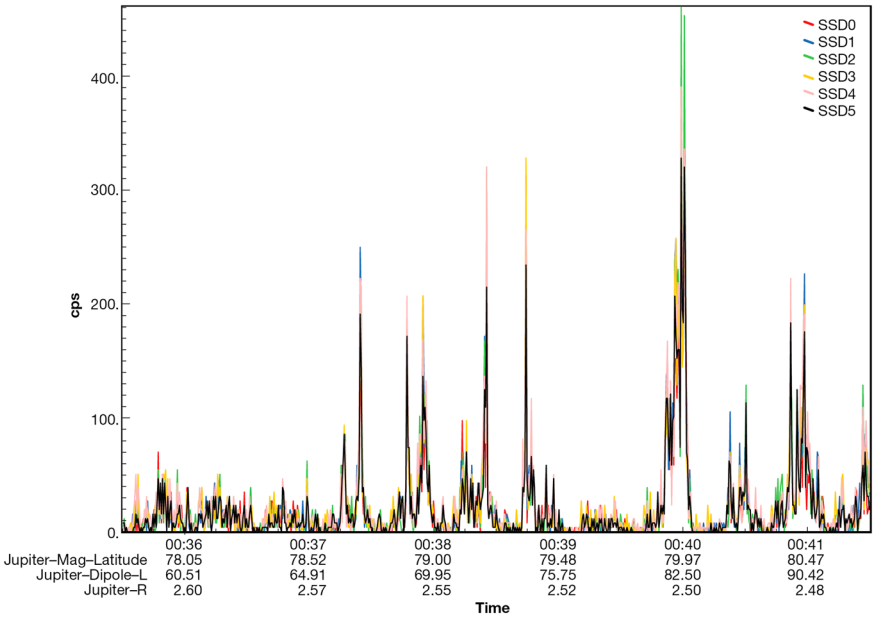

Figure 6. Expansion of several minutes of data obtained on 2017-192, during PJ7. The count rate of JEDI-A180 ion singles are shown with no averaging for the 6 min between 00:35:30 and 00:41:30.

Figure 6 shows another example of these intense beams observed during PJ7. Here we again display the JEDI-A180 ion SSD singles, but now for a much shorter period of time. Without averaging the data, it is easier to observe how the beam is detected by JEDI at approximately the spacecraft spin period of 30 s. Sometimes, there is no strong upward beam, for example, in the 30 s prior to the event near 00:40. When the FOVs point into the beam, all the SSDs detect similar count rates, even though some of them are measuring local pitch angles that are well away from the beam direction.

5. Discussion

Ebert et al. (2017) described differences between bi-directional electron beams over Jupiter's polar regions and upward beams. They noted that the latter tend to be narrow in energy, with peak components that could be as high as a few hundred keV, pointing to the analysis of inverted-V structures in the work of Clark et al. (2017). This paper and the earlier work of Mauk et al. (2017a, 2017b) extend the energy range of the electrons in the upward electron beams. The presence of the feature near 160 keV that often occurs during the observation of these beams shows that electrons above 420 keV are present and that the count rate associated with these electrons dominates the energy-time spectrograms. We argue here that the beams have substantial contributions above 1.2 MeV due to the band and the low count rates between the band and 1.2 MeV.

In Table 1, we list times during which Juno observes continuous periods of intense upward beams, through PJ8. We do not list all the times that satisfied the metric we discussed above because some are very brief. The

Table 1
Times of Intense Upward Beam Observations Using the Convergence of the JEDI-A180 Small Pixel Ion Count Rates as the Metric During Beam Times

Year-day	PJ number	Times of longer events	Related figures in this paper
2016–240	PJ1	Brief events, e.g., just prior to 12:00	
2016–346	PJ3	15:37–16:19	See Figure 2
2017–033	PJ4	12:00–12:22 (inb) 14:07–14:35 (outb)	See Figures 3–5, and 7
2017–086	PJ5	Brief events, e.g., ~08:26–08:36	
2017–139	PJ6	No events?	
2017–192	PJ7	00:37–01:12	See Figure 6
2017–244	PJ8	20:45–21:11	

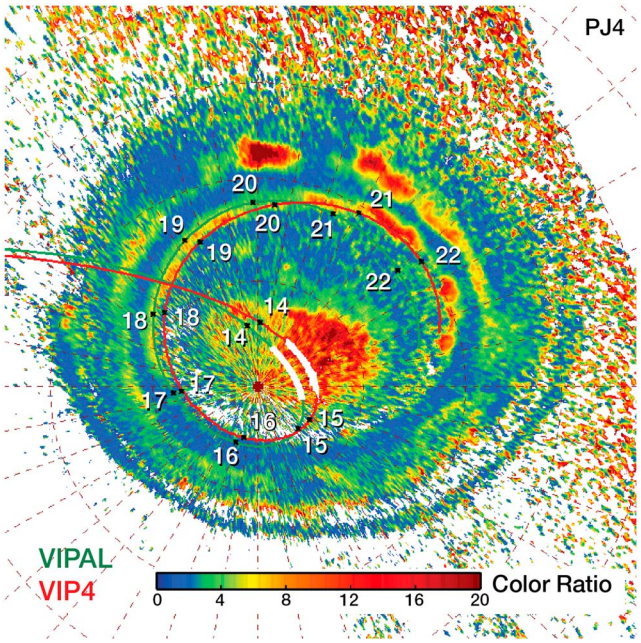

Figure 7. Color ratio created from Juno Ultraviolet Spectrograph data obtained over the southern hemisphere of Jupiter during PJ4. The Juno footprint is traced to the surface of Jupiter using two magnetic field models (red and green lines). The swirl region (red) near the center of the plot is briefly magnetically connected to Juno in both models. The white segments of the trajectory footprints indicate the times when Jupiter Energetic particle Detector Instrument saw the most intense upward electron beams.

times below are based on JEDI data that show JEDI-A180 small ion pixel SSD singles rates that are all approximately the same, suggesting an internal scattering process or the presence of electrons with high enough energies to penetrate the collimator blades or the housing. During these times, a band near 160 keV appears when JEDI looks close to the magnetic field direction, the band can often spread in energy above and below 160 keV, nonbeam pitch angles register significant counts, and the SSD singles rates tend to be higher.

At this time, we do not have an explanation for the mechanism that accelerates electrons to energies characteristic of these beams. The Ulysses spacecraft also detected energetic electron bursts, with energies of ~1 to >16 MeV, attributed to an acceleration or injection region at low altitude near Jupiter's south pole (McKibben, Simpson, & Zhang, 1993). Specific signatures were observed in ultraviolet observations of the polar atmosphere during the times of the most intense beams.

Mauk et al. (2017b) showed that the features JEDI observed on 2016–346 at 15:40 appeared to connect to a UV polar auroral arc along the boundary of the swirl region. After this point, Juno crossed onto field lines connected with the UV swirl region and during this interval, the high energy upward beams we are reporting on here were observed. Indeed, there appears to be an association between the most intense upward beams described here and the swirl region of the aurora.

In Figure 7, we show a polar projection of the color ratio measured by the Juno-UVS instrument (Gladstone et al., 2017) between 14:07:02 and 14:34:58 on 2017-033. This quantity is the ratio of the brightness in the 155–162 nm range over the brightness in the 125–130 nm range. The latter wavelength range being strongly absorbed by CH_4, the color ratio increases when the altitude of the emission decreases. Since higher energy particles precipitate deeper into the atmosphere, the color ratio is thus a proxy for the energy of the precipitating particles. The red and green plots are the projection of the Juno trajectory along the VIP4 (Connerney et al., 1998) and VIPAL (Hess et al., 2011) magnetic field models during the outbound segment of PJ4. The white portions of the trajectory footprint lines correspond to times JEDI sees intense upward electron beams. These are within the swirl region (red in the color ratio).

Times when the JEDI-A180 small pixel ion sensors record rates similar to each other (despite the witness shields) are in the high-latitude portions of the radiation belts and over the swirl region. We have found good correlation between the swirl times from UVS and the very intense beams of JEDI (with few or no counterexamples to date). The swirl region has been described as a patchy area of low brightness and high absorption in the polar region that presumably connects to the most "open" magnetic field lines connecting to Jupiter (Bonfond et al., 2017). But as noted above, more work on the relevant physical processes needs to be done to link these interesting observations.

Acknowledgments
We appreciate the assistance of J. Peachey and L. Brown with data processing. B. B. was funded by the Fund for Scientific Research (F.R.S.-FNRS). W. R. D. is supported by a Science and Technology Facilities Council (STFC) research grant to University College London (UCL), an SAO fellowship to Harvard-Smithsonian Centre for Astrophysics, and by European Space Agency (ESA) contract 4000120752/17/NL/MH. Juno/JEDI data are available through NASA's Planetary Data System (PDS) for the cruise and early perijoves.

References

Allegrini, F., Bagenal, F., Bolton, S., Connerney, J., Clark, G., Ebert, R. W., et al. (2017). Electron beams and loss cones in the auroral regions of Jupiter. *Geophysical Research Letters*, *44*, 7131–7139. https://doi.org/10.1002/2017GL073180

Armstrong, T. P., Paonessa, M., Brandon, S. T., Krimigis, S. M., & Lanzerotti, L. J. (1981). Low energy charged particle observations in the 5–20 R_J region of the Jovian magnetosphere. *Journal of Geophysical Research*, *86*(A10), 8343–8355. https://doi.org/10.1029/JA086iA10p08343

Becker, H. N., Santos-Costa, D., Jorgensen, J. L., Denver, T., Adriani, A., Mura, A., et al. (2017). Observations of MeV electrons in Jupiter's innermost radiation belts and polar regions by the Juno radiation monitoring investigation: Perijoves 1 and 3. *Geophysical Research Letters*, *44*, 4481–4488. https://doi.org/10.1002/2017GL073091

Bonfond, B., Gladstone, G. R., Grodent, D., Greathouse, T. K., Versteeg, M. H., Hue, V., et al. (2017). Morphology of the UV aurorae Jupiter during Juno's first perijove observations. *Geophysical Research Letters*, *44*, 4463–4471. https://doi.org/10.1002/2017GL073114

Branduardi-Raymont, G., Bhardwaj, A., Elsner, R. F., Gladstone, G. R., Ramsay, G., Rodriguez, P., et al. (2007). A study of Jupiter's aurorae with XMM-Newton. *Astronomy and Astrophysics*, *463*, 761–774. https://doi.org/10.1051/0004-6361:20066406

Bunce, E. J., Cowley, S. W. H., & Yeoman, T. K. (2004). Jovian cusp processes: Implications for the polar aurora. *Journal of Geophysical Research*, *109*, A09S13. https://doi.org/10.1029/2003JA010280

Clark, G., Mauk, B. H., Paranicas, C., Haggerty, D., Kollmann, P., Rymer, A., et al. (2017). Energetic particle signatures of magnetic field-aligned potentials over Jupiter's polar regions. *Geophysical Research Letters*, *44*, 8703–8711. https://doi.org/10.1002/2017GL074366

Connerney, J. E. P., Acuna, M. H., Ness, N. F., & Satoh, T. (1998). New models of Jupiter's magnetic field constrained by the Io flux tube footprint. *Journal of Geophysical Research*, *103*, 11,929–11,940. https://doi.org/10.1029/97JA03726

Connerney, J. E. P., Adriana, A., Allegrini, F., Bagenal, F., Bolton, S. J., Bonfond, B., et al. (2017). Jupiter's magnetosphere and aurorae observed by the Juno spacecraft during its first polar orbits. *Science*, *356*(6340), 826–832. https://doi.org/10.1126/science.aam5928

Connerney, J. E. P., Benn, M., Bjarno, J. B., Denver, T., Espley, J., Jorgensen, J. L., et al. (2017). The Juno magnetic field investigation. *Space Science Reviews*, *213*, 39–138. https://doi.org/10.1007/s11214-017-0334-z

Ebert, R., Allegrini, F., Bagenal, F., Bolton, S. J., Connerney, J. E. P., Clark, G., et al. (2017). Spatial distribution and properties of 0.1–100 keV electrons in Jupiter's polar auroral region. *Geophysical Research Letters*, *44*, 9199–9207. https://doi.org/10.1002/2017GL075106

Elsner, R. F., Lugaz, N., Waite, J. H., Cravens, T. E., Gladstone, G. R., Ford, P., et al. (2005). Simultaneous Chandra X-ray, Hubble Space Telescope ultraviolet, and Ulysses radio observations in Jupiter's aurora. *Journal of Geophysical Research*, *110*, A01207. https://doi.org/10.1029/2004JA010717

Gladstone, G. R., Persyn, S. C., Eterno, J. S., Walther, B. C., Slater, D. C., Davis, M. W., et al. (2017). The ultraviolet spectrograph on NASA's Juno mission. *Space Science Reviews*, *213*, 447–473. https://doi.org/10.1007/s11214-014-0040-z

Grodent, D., Clarke, J. T., Waite, J. H. Jr., Cowley, S. W. H., Gerard, J.-C., & Kim, J. (2003). Jupiter's polar auroral emissions. *Journal of Geophysical Research*, *108*(A10), 1366. https://doi.org/10.1029/2003JA010017

Haggerty, D. K., Mauk, B. H., Paranicas, C. P., Clark, G., Kollmann, P., Rymer, A. M., et al. (2017). Juno/JEDI observations of 0.01 to >10 MeV energetic ions in the Jovian auroral regions: Anticipating a source for polar x-ray emission. *Geophysical Research Letters*, *44*, 6476–6482. https://doi.org/10.1002/2017GL072866

Hess, S. L. G., Bonfond, B., Zarka, P., & Grodent, D. (2011). Model of the Jovian magnetic field topology constrained by the Io auroral emissions. *Journal of Geophysical Research*, *116*, A05217. https://doi.org/10.1029/2010JA016262

Kollmann, P., Paranicas, C., Clark, G., Mauk, B. H., Haggerty, D. K., Rymer, A. M., et al. (2017). A heavy ion and proton radiation belt inside of Jupiter's rings. *Geophysical Research Letters*, *44*, 5259–5268. https://doi.org/10.1002/2017GL073730

Lanzerotti, L. J., Armstrong, T. P., Gold, R. E., Anderson, K. A., Krimigis, S. M., Lin, R. P., et al. (1992). The hot plasma environment at Jupiter: Ulysses results. *Science*, *257*(5076), 1518–1524. https://doi.org/10.1126/science.257.5076.1518

Mauk, B. H., Haggerty, D. K., Jaskulek, S. E., Schlemm, C. E., Brown, L. E., Cooper, S. A., et al. (2017). The Jupiter Energetic Particle Detector Instrument (JEDI) investigation for the Juno mission. *Space Science Reviews*, *213*(1-4), 289–346. https://doi.org/10.1007/s11214-013-0025-3

Mauk, B. H., Haggerty, D. K., Paranicas, C., Clark, G., Kollmann, P., Rymer, A. M., et al. (2017a). Juno observations of energetic charged particles over Jupiter's polar regions: Analysis of mono- and bi-directional electron beams. *Geophysical Research Letters*, *44*, 4410–4418. https://doi.org/10.1002/2016GL072286

Mauk, B. H., Haggerty, D. K., Paranicas, C., Clark, G., Kollmann, P., Rymer, A. M., et al. (2017b). Discrete and broadband electron acceleration generating Jupiter's uniquely powerful aurora. *Nature*, *549*(7670), 66–69. https://doi.org/10.1038/nature23648

McKibben, R. B., Simpson, J. A., & Zhang, M. (1993). Impulsive bursts of relativistic electrons discovered during Ulysses' traversal of Jupiter's dusk magnetosphere. *Planetary and Space Science*, *41*(11-12), 1041–1058. https://doi.org/10.1016/0032-0633(93)90108-E

Paranicas, C., Mauk, B. H., Haggerty, D. K., Clark, G., Kollmann, P., Rymer, A. M., et al. (2017). Radiation near Jupiter detected by Juno/JEDI during PJ1 and PJ3. *Geophysical Research Letters*, *44*, 4426–4431. https://doi.org/10.1002/2017GL072600